Molecular Neurobiology (2023) 60:864–874
https://doi.org/10.1007/s12035-022-03122-9

Toll-Like Receptor 4 Signaling in Neurons Mediates Cerebral Ischemia/Reperfusion Injury

Liang Liu[1] · Tian-Ce Xu[1] · Zi-Ai Zhao[1] · Nan-Nan Zhang[1] · Jing Li[1] · Hui-Sheng Chen[1]

Received: 1 September 2022 / Accepted: 4 November 2022 / Published online: 16 November 2022

Abstract

In microglia, Toll-like receptor 4 (TLR4) is well known to contribute to neuroinflammatory responses following brain ischemia. TLR4 is also expressed in neurons and can mediate the conduction of calcium (Ca^{2+}) influx, but the mechanistic link between neuronal TLR4 signaling and brain ischemic injury is still poorly understood. Here, primary neuronal cell cultures from TLR4 knockout mice and mice with conditional TLR4 knockout in glutamatergic neurons ($TLR4^{cKO}$) were used to establish ischemic models in vitro and in vivo, respectively. We found that deleting TLR4 would reduce the neuronal death and intracellular Ca^{2+} increasement induced by oxygen and glucose deprivation (OGD) or lipopolysaccharide treatment. Infarct volume and functional deficits were also alleviated in $TLR4^{cKO}$ mice following cerebral ischemia/reperfusion (I/R). Furthermore, TLR4 and N-methyl-D-aspartate receptor subunit 2B (NMDAR2B) were colocalized in neurons. Deletion of TLR4 in neurons rescued the upregulation of phosphorylated NMDAR2B induced by ischemia via Src kinase in vitro and in vivo. Downstream of NMDAR2B signaling, the interaction of neuronal nitric oxide synthase (nNOS) with postsynaptic density protein-95 (PSD-95) was also disrupted in $TLR4^{cKO}$ mice following cerebral I/R. Taken together, our results demonstrate a novel molecular neuronal pathway in which TLR4 signaling in neurons plays a crucial role in neuronal death and provide a new target for neuroprotection after ischemic stroke.

Keywords Toll-like receptor 4 · Ischemic stroke · Neuronal death · N-Methyl-D-aspartate receptor · Neuroprotection

Abbreviations

TLR4	Toll-like receptor 4
Ca^{2+}	Calcium
$TLR4^{cKO}$	Conditional knockout mice of TLR4 in glutamatergic neurons
OGD	Oxygen and glucose deprivation
I/R	Ischemia/reperfusion
NMDAR2B	N-methyl-D-aspartate receptor subunit 2B
nNOS	Neuronal nitric oxide synthase
PSD-95	Postsynaptic density protein-95
LPS	Lipopolysaccharide
VGLUT2	Vesicular glutamate transporters 2
MCAO	Middle cerebral artery occlusion
WT	Wild type
TTC	Triphenyl tetrazolium chloride
FJB	Fluoro-Jade B

✉ Hui-Sheng Chen
chszh@aliyun.com

[1] Department of Neurology, The General Hospital of Northern Theater Command, No. 83 Wenhua Street, Shenhe District, ShenyangLiaoning 110016, China

Introduction

Neuroimmune signaling that includes the innate immunity receptor Toll-like receptor 4 (TLR4) has been well demonstrated to play critical roles in neuropathology following ischemia/reperfusion (I/R) injury [1]. While previous studies have primarily focused on the inflammatory response mediated by TLR4 on microglia in the pathogenesis of stroke [2, 3], TLR4 was recently found to also be expressed on neurons and involved in cerebral I/R injury [4]. However, the mechanistic link between neuronal TLR4 signaling and I/R injury is still poorly understood.

Immediately following ischemia, glutamate accumulates rapidly at synapses, which stimulates N-methyl-D-aspartate receptors (NMDARs) to induce a large amount of calcium (Ca^{2+}) influx through the NMDAR channels, resulting in irreversible neuronal death [5, 6]. NMDAR Ca^{2+} permeability is increased by the excessive activation of Tyr phosphorylation of the NMDAR subunit 2B (NMDAR2B) [7]. Interestingly, lipopolysaccharide (LPS), a TLR4 agonist, increases cytosolic [Ca^{2+}] and promotes apoptosis in aged rat hippocampal cultures [8]. Additionally, TLR4 signaling

has been shown to enhance Ca^{2+} permeability in neuronal cell bodies through NMDA receptors in hippocampal cultures [9]. However, the possible interactions of neuronal TLR4 and NMDAR2B following ischemia/reperfusion injury have not yet been assessed.

In this work, TLR4 conditional knockout mice and primary neuronal cell culture from TLR4 knockout mice were used to establish ischemic stroke models in vivo and in vitro, in order to elucidate the mechanism between neuronal TLR4 and NMDAR2B in the pathogenesis of ischemic stroke.

Materials and Methods

Animals

$TLR4^{fl}$ [B6(Cg)-Tlr4tm1.1Karp/J, IMSR_JAX: B004319] and Vglut2-ires-Cre knock-in [B6J.129S6(FVB)-Slc17a6tm2(cre)Lowl/MwarJ, IMSR_JAX: B004320] mouse lines were obtained from the Jackson Laboratory (Bar Harbor, ME). To delete TLR4 from all VGLUT2 (vesicular glutamate transporters 2; glutamatergic) neurons ($TLR4^{cKO}$), the Cre driver line was crossed with $TLR4^{fl}$ mice. Mice were genotyped by PCR. $TLR4^{-/-}$ mice were obtained from The Jackson Laboratories (Strain Name: C57BL/10ScNJ). Male mice were used in all studies. All animals were housed in a controlled environment on a 12-h light/12-h dark illumination schedule and were fed a standard pellet diet with water provided ad libitum. All experimental procedures were performed in accordance with approved principles of the Animal Ethics Committee of the General Hospital of Northern Theater Command (ethical approval number: 2020–008) and followed the ARRIVE (Animal Research: Reporting of In Vivo Experiments) guidelines.

Cerebral Ischemia/Reperfusion Injury Model

Cerebral ischemia/reperfusion (I/R) injury was induced by intraluminal middle cerebral artery occlusion (MCAO) and reperfusion, as described previously [10]. Briefly, the mice were first anesthetized using 5.0% isoflurane. The left common carotid artery (CCA), internal carotid artery (ICA), and external carotid artery (ECA) were exposed by a midline incision. Microvascular aneurysm clips were applied to the right CCA and the ICA. A coated 6–0 filament (Doccol, Redlands, CA) was introduced into an arteriotomy hole, fed distally into the ICA, and advanced a predetermined distance of 8 mm from the carotid bifurcation toward the MCA. The filament was left in place for 90 min and then withdrawn. The collar suture at the base of the ECA stump was then tightened. The skin incision was closed and anesthesia was discontinued. Mice in the sham group underwent neck dissection and coagulation of the external carotid artery, but the middle cerebral artery was not occluded. After surgery, individual animals were returned to their cages with free access to water and food. All experiments were performed in a randomized fashion by investigators blinded to treatment groups.

Cell Culture and Oxygen–Glucose Deprivation

As reported in previous studies, cortices were isolated from embryonic day 16 (E16) wild-type (WT) mice and TLR4 knockout ($TLR4^{-/-}$) mice [11]. Cells were dissociated and purified using a papain dissociation kit (Worthington Biochemical Corporation). Primary cortical neurons were cultured in neurobasal media (containing 4.5 g/l glucose, supplemented with GlutaMAX and B27; Life Technologies) for 18 days. As described in a previous study [10], oxygen and glucose deprivation (OGD) treatment was performed by removing the culture medium and replacing it with D-Hank's solution (Life Technologies); the cultures were then incubated in an anaerobic atmosphere of 95% N_2 and 5% CO_2 at 37 °C for 1 h. OGD was terminated by replacing the D-Hank's solution with a normal culture medium and returning the cells to a normoxic incubator. Control plates were maintained in the normoxic incubator during the OGD interval. Assays were conducted using 96-well microtiter plates. Cell viability was assessed using a CCK-8 assay (Dojindo Co. Tokyo, Japan) according to the manufacturer's protocols. Cell viability is expressed as a percentage of the control.

Neurobehavioral Evaluation and Assessment of Cerebral Infarct Volume

Neurological deficit scores were scored by an observer blinded to the experimental groups using a previously described method [12]. Briefly, the mouse scoring system was as follows: grade 0, no observable neurological deficits; grade 1, failed to extend the right forepaw; grade 2, circled to the right; grade 3, fell to the right; grade 4, could not walk spontaneously; and grade 5, dead.

The cerebral infarct volume was determined using a previously described method [13]. At 24.5 h after the cerebral ischemia/reperfusion operation, the animals were sacrificed and perfused with ice-cold PBS via the ascending aorta. The brains were cut into five 2-mm-thick coronal sections. The slices were stained with a 2% triphenyl tetrazolium chloride (TTC) solution (Sigma−Aldrich) for 15 min at 37 °C, followed by fixation in 4% paraformaldehyde. We measured the entire area of the prosencephalon and the cerebral infarct with Image-Pro Plus 5.0 image processing software (Media Cybernetics). The lesion volume was calculated using the formula $V = t^*(A1 + A2 + \ldots An)$, where V is the volume of the infarct or prosencephalon, t is the thickness of the

slice, and *A* is the infarct size and the volumetric ratio of the cerebral infarct (cerebral infarction volume/prosencephalon volume).

TUNEL and Fluoro-Jade B Staining

TUNEL and Fluoro-Jade B (FSJB) staining were performed according to the manufacturer's protocols. The animals were deeply anesthetized and perfused with cold PBS followed by 4% paraformaldehyde through the ascending aorta, and the brains were sectioned coronally. TUNEL staining was performed using an In Situ Cell Death Detection Kit (Roche, Indianapolis, IN). Cell degeneration was detected using an FJB Staining Kit (Millipore, Billerica, MA). Sections were observed and photographed under a confocal laser scanning microscope (Leica, Germany). The number of TUNEL- and FJB-positive neurons was counted and calculated using Image-Pro Plus v6.0 image analysis software (Media Cybernetics, USA).

Measurement of Intracellular Ca^{2+} Ions

Intracellular Ca^{2+} ion changes were assessed using a sensitive Ca^{2+} indicator, Fluo-4-AM (Invitrogen, Carlsbad, CA). Neuronal cells were cultured on collagen-coated confocal dishes with culture media containing 1% FBS and were loaded with 4 μM Fluo-4 AM dye for 40 min at 37 °C. After loading, the cells were washed with Hanks' solution three times. Intracellular calcium dynamics were visualized using a confocal microscope (Leica, Germany) with 488-nm excitation and 530-nm emission. Lipopolysaccharide (LPS) was added during the times indicated in the figures. Images were taken every 3 s, and each cell was observed for 5 min. The changes in the fluorescence intensity within the selected cells were quantitatively analyzed using TCS-SP2 confocal laser-scanning microscopy (CLSM) software. For intracellular Ca^{2+} ion change calculations, the method described by Moon et al. [14] was used with the following equation: $[Ca^{2+}]i = Kd(F - F_{min})/(F_{max} - F)$, where Kd is 345 nM for Fluo-4, and F is the observed fluorescence intensity in real time. Each tracing was calibrated for the maximal (F_{max}) by adding ionomycin (2 μM) and for the minimum intensity (F_{min}) by adding EGTA (5 mM) at the end of each measurement.

Coimmunoprecipitation and Western Blotting

Mice were sacrificed 24 h after the induction of cerebral ischemia, and the brains were removed. Following 3 h of OGD, the cells were collected. The cerebral cortex tissues or cells were homogenized in RIPA buffer (Beyotime Institute of Biotechnology) and spun down at 13,000 rpm for 10 min, and then the supernatants were collected. The protein concentration was determined using a BCA Kit (Beyotime Institute of Biotechnology). For coimmunoprecipitation, the separated proteins were incubated with polyclonal rabbit anti-nNOS (1:100, Affinity BioReagents) or anti-PSD-95 (1:100, Cell Signaling Technology) overnight at 4 ℃, followed by the addition of 40 ml of Protein G-Sepharose (Sigma) for 3 h at 4 ℃. Proteins were analyzed by immunoblotting.

The separated proteins were transferred onto a 12% SDS–polyacrylamide gel at 80 V for 120 min and then transferred to PVDF membranes. Blotting membranes were blocked in a solution (5% nonfat dried milk powder dissolved in TBST buffer) at room temperature for 3 h, and then washed three times. Next, the membranes were incubated overnight at 4 °C with primary antibodies against nNOS (1:5000, Affinity BioReagents), PSD-95 (1:5000, Cell Signaling Technology), NMDAR2B (1:5000, Affinity BioReagents), phospho-NMDAR2B (Ser1303, 1:5000, Affinity BioReagents), Src (1:5000, Affinity BioReagents), and β-actin (1:5000, Affinity BioReagents). The membranes were washed and incubated for 2 h with horseradish peroxidase–conjugated secondary antibody (1:1000, Santa Cruz Biotechnology). The bands were scanned and analyzed using a chemiluminescence system (Bio-Rad Laboratories Inc.) [15, 16].

Immunofluorescence

According to our previous methods [17], mice were deeply anesthetized with an overdose of isoflurane and transcardially perfused with 0.01 M phosphate-buffered saline (PBS, pH 7.4) for 5–10 min followed by 4% paraformaldehyde in 0.1 M PBS for 15–20 min. Whole brains were removed and postfixed with 4% paraformaldehyde for 24 h followed by 30% sucrose solution with 4% paraformaldehyde at 4 °C. Coronal cryosections were collected. Primary cortical neurons were fixed with 4% p-formaldehyde. The sections were incubated with the primary antibodies in 1% bovine serum albumin overnight at 4 °C: rabbit anti-β III Tubulin (1:1000, Abcam), mouse anti-NMDAR2B (1:1000, Abcam), and goat anti-TLR4 (1:500, Santa Cruz). The Cy3-, 647-, or 488-conjugated secondary antibodies (1:500, Jackson ImmunoResearch) were subsequently added (2 h, 37 °C). Sections were counterstained with 4′,6-diamidino-2-phenylindole (Sigma−Aldrich, St. Louis, MO, USA) and were viewed using a confocal laser-scanning microscope (Leica TCS-SP2, Heidelberg, Germany) and analyzed with Leica imaging software.

Statistical Analysis

All data are presented as the mean ± SEM and were analyzed using SPSS 20.0 software (SPSS Inc., Chicago, IL, USA). Data analyses were performed using one-way ANOVAs,

and significant effects were evaluated with Tukey's post hoc tests. Moreover, to compare means between two groups, a two-tailed, unpaired Student's *t*-test was used. A value of $p < 0.05$ was considered statistically significant.

Results

Neurons Deficient in TLR4 Are Resistant to Death and Intracellular Ca^{2+} Increase Induced by OGD or LPS Treatment

Primary mouse cortical neurons have been found to express TLR2, TLR3, TLR4, and TLR8, but the function of TLRs in neurons has not been fully evaluated [4, 18]. To examine whether neuronal TLR4 signaling plays a pivotal role during an ischemic injury in vitro, primary mouse cortical neurons from both wild-type (WT) and $TLR4^{-/-}$ mice were used (Suppl. Fig. S1) and treated with oxygen and glucose deprivation (OGD). The results showed that neuronal TLR4 knockout significantly reduced lactate dehydrogenase release from cultured neurons treated with OGD compared with WT neurons (Fig. 1a). Moreover, neurons from $TLR4^{-/-}$ mice significantly increased OGD-induced cell viability, as shown by a CCK-8 assay (Fig. 1b). We also examined the effects of neuronal TLR4 signaling on cell apoptosis following OGD by TUNEL staining and found that neurons from $TLR4^{-/-}$ mice were significantly more resistant to OGD-induced cell apoptosis than neurons from WT mice (Fig. 1c, d). Therefore, these results suggest that OGD-induced apoptosis in cultured neurons may depend on neuronal TLR4.

It has been reported that an increase in $[Ca^{2+}]i$ is a central event in the neuronal death process [19]. Thus, we examined the role of neuronal TLR4 signaling on intracellular Ca^{2+} levels in neurons following treatment with lipopolysaccharide (LPS), a selective TLR4 antagonist. Cells were

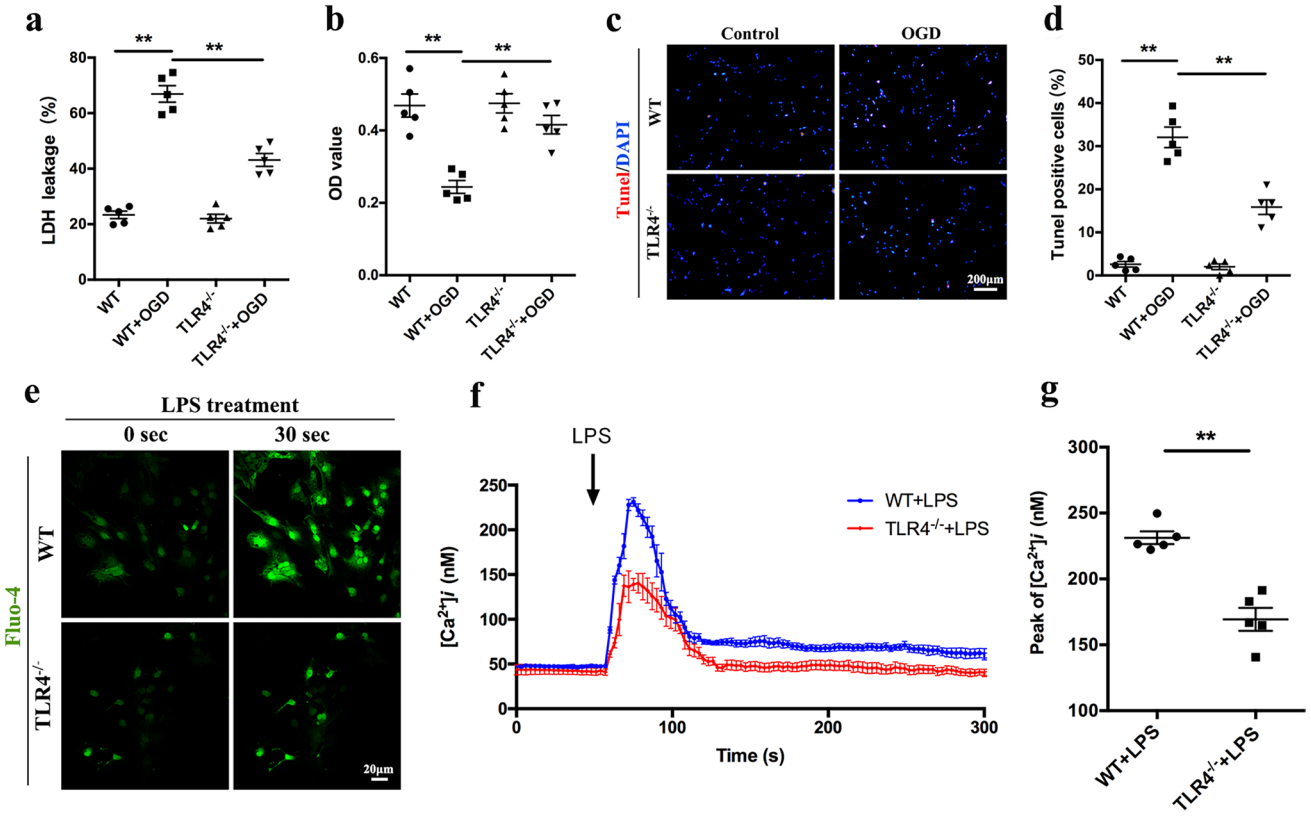

Fig. 1 Neurons deficient in the TLR4 receptor are resistant to OGD-induced apoptosis and LPS-induced intracellular Ca^{2+} increase. **a**, **b** Cultured cortical neurons from WT mice and TLR4 knockout mice were exposed to oxygen and glucose deprivation for 30 min, and lactate dehydrogenase (LDH) release (**a**) and cell viability (**b**) were measured ($n = 5$). **c**, **d** Cell survival was quantified by TUNEL staining following OGD treatment. **e** Cultured neurons were exposed to fluo-4 AM, and the changes in the intracellular Ca^{2+} levels were evaluated using confocal microscopy. The green fluorescence (fluo-4 AM) intensity, which represents the $[Ca^{2+}]i$ (intracellular calcium) concentration, changes time-dependently in neurons. **f** $[Ca^{2+}]i$ was measured for 300 s in five independent experiments. The results showed that the average kinetics of Ca^{2+} in the WT + LPS groups were greater than those in the $TLR4^{-/-}$ + LPS groups ($n = 5$). LPS treatment is shown by arrows. **g** Bar graphs represent the peak value of the neuronal Ca^{2+} response to LPS treatment ($n = 5$). Values are represented as the mean ± SEM. $^{**}P < 0.01$

loaded with Fluo-4 AM and subjected to fluorescence Ca^{2+} imaging. The results showed that LPS treatment rapidly increased the intracellular Ca^{2+} levels in the WT cultured neurons, although the increase was transient, while LPS-induced $[Ca^{2+}]i$ oscillation was abolished in neurons from $TLR4^{-/-}$ mice (Fig. 1e–g). These results suggest that TLR4 is involved in Ca^{2+} responses to LPS in neurons.

Deletion of TLR4 from Vglut2 Neurons Alleviates Ischemic Neuronal Death and Functional Deficits in a Mouse Stroke Model

To evaluate whether TLR4 is critically involved in neuronal damage and functional deficits in a mouse stroke model, a middle cerebral artery occlusion/reperfusion mouse model was used. $Tlr4^{fl/fl}$ mice were mated with $Vglut2^{ires-Cre/+}$ mice to delete TLR4 from all VGLUT2 (glutamatergic) neurons ($Vglut2^{ires-Cre/+} + Tlr4^{fl/fl}$, $TLR4^{cKO}$). After such mattings, ~ 50% of all offspring are controls (i.e., $Tlr4^{fl/fl}$ mice) and ~ 50% have a deletion of TLR4 in glutamatergic neurons (i.e., $Vglut2^{ires-Cre/+} + Tlr4^{fl/fl}$ mice). Mice were genotyped by PCR (Suppl. Fig. S2). Before MCAO, mouse body weight was measured (Suppl. Fig. S3a), and the movement was evaluated using an open-field test (Suppl. Fig. S3b, c). Next, $TLR4^{cKO}$ and control ($Tlr4^{fl/fl}$) mice underwent focal cerebral ischemia with middle cerebral artery occlusion for 90 min. Twenty-four hours after reperfusion, brain sections were stained with TUNEL and Fluoro-Jade B (FJB), an in situ cell death detection kit and a marker for degenerating neurons, respectively. The CA1 area of the hippocampus, the cortex, and the striatum were examined due to their vulnerability to transient global ischemic insult [20]. We found that deletion of TLR4 in glutamatergic ($VGLUT2^{+}$) neurons produced a dramatic reduction in TUNEL- and FJB-positive cells compared with control mice (Fig. 2a–d). Moreover, we tested neurological outcome and infarct size at 24 and 24.5 h after reperfusion, respectively. Brain infarction was analyzed using TTC staining. We found that brain infarct volume was much lower in $TLR4^{cKO}$ mice than in control mice (Fig. 2e, f), and the reduction in infarction volume was associated with improvement in neurological scores in $TLR4^{cKO}$ mice (Fig. 2g). Collectively, these results further support the critical role of neuronal TLR4 signaling in cerebral I/R injury and highlight the possible involvement of glutamatergic neurons.

TLR4 and NMDAR2B Coexpression in Neurons Respond to Ischemic Stimulation

Given the pivotal role of neuronal TLR4 signaling in intracellular Ca^{2+} increase responses to LPS and neuronal death during an ischemic injury in vitro and in vivo and the key involvement of N-methyl-D-aspartate receptor subunit 2B (NMDAR2B) in neuronal hyperexcitability [21], we hypothesized that TLR4 and the target NMDAR2B would colocalize in the same neuronal structures. To test this hypothesis, we used immunofluorescent staining with differentially labeled secondary antibodies and found that TLR4 and NMDAR2B were coexpressed in neurons and responded to ischemic stimulation in vitro and in vivo (Fig. 3a, b).

Neurons Deficient in TLR4 Rescue the Upregulation of Phosphorylated NMDAR2B Induced by OGD Treatment Through Src Kinase

Having demonstrated that genetic deletion of neuronal TLR4 alleviates ischemia-induced injury and that TLR4 is coexpressed with NMDAR2B in neurons, we next examined the functional impacts of TLR4 deletion on NMDAR2B toxicity following OGD treatment. Since NMDAR channel-gating properties are regulated by Src family kinases through phosphorylation of the NMDAR2B subunit [22], the levels of Src kinase, NMDAR2B, and phosphorylation at Ser-1303 (p-NMDAR2B) in neurons after OGD treatment were evaluated using Western blotting (Fig. 4a). The results showed that the expression of p-NMDAR2B in neurons increased significantly following OGD treatment, which was not observed in $TLR4^{-/-}$ neurons (Fig. 4b). Moreover, given that nNOS is a downstream signal of NMDAR2B and contributes to glutamate-induced neuronal death [23], we also measured nNOS expression. The results showed that the deletion of neuronal TLR4 rescued the increase in nNOS expression induced by OGD (Fig. 4c). The total level of Src kinase was not changed by the treatments (Fig. 4d).

Given that Src family kinases have been reported to play a crucial role in NMDA-induced Ca^{2+} influx and phosphorylation of the NMDAR2B subunit following activation of the IL-1β/IL-1R1 axis in neurons [24] and that IL-1R1 and TLR4 have a similar cytosolic Toll/IL-1 receptor domain [25], we further investigated the roles of Src kinase in OGD-induced NMDAR2B toxicity mediated by neuronal TLR4 signaling. To this end, we added 10 μM 4-amino-5-(4-chlorophenyl)-7-(t-butyl) pyrazolo [3,4-d] pyrimidine (PP2), a selective antagonist of Src family kinases [26], 30 min before OGD treatment, and observed that PP2 significantly increased neuronal viability and reduced LDH release and neuronal apoptosis (Fig. 4e–h). PP2 induced a significant decrease in the expression of p-NMDAR2B and nNOS in neurons following OGD (Fig. 4i–k). Furthermore, PP2 prevented the enhancement of the NMDA-induced Ca^{2+} response caused by LPS treatment in neurons (Fig. 4l, m). Taken together, these findings suggest that neurons deficient in TLR4 may rescue NMDAR2B toxicity induced by OGD via Src kinase.

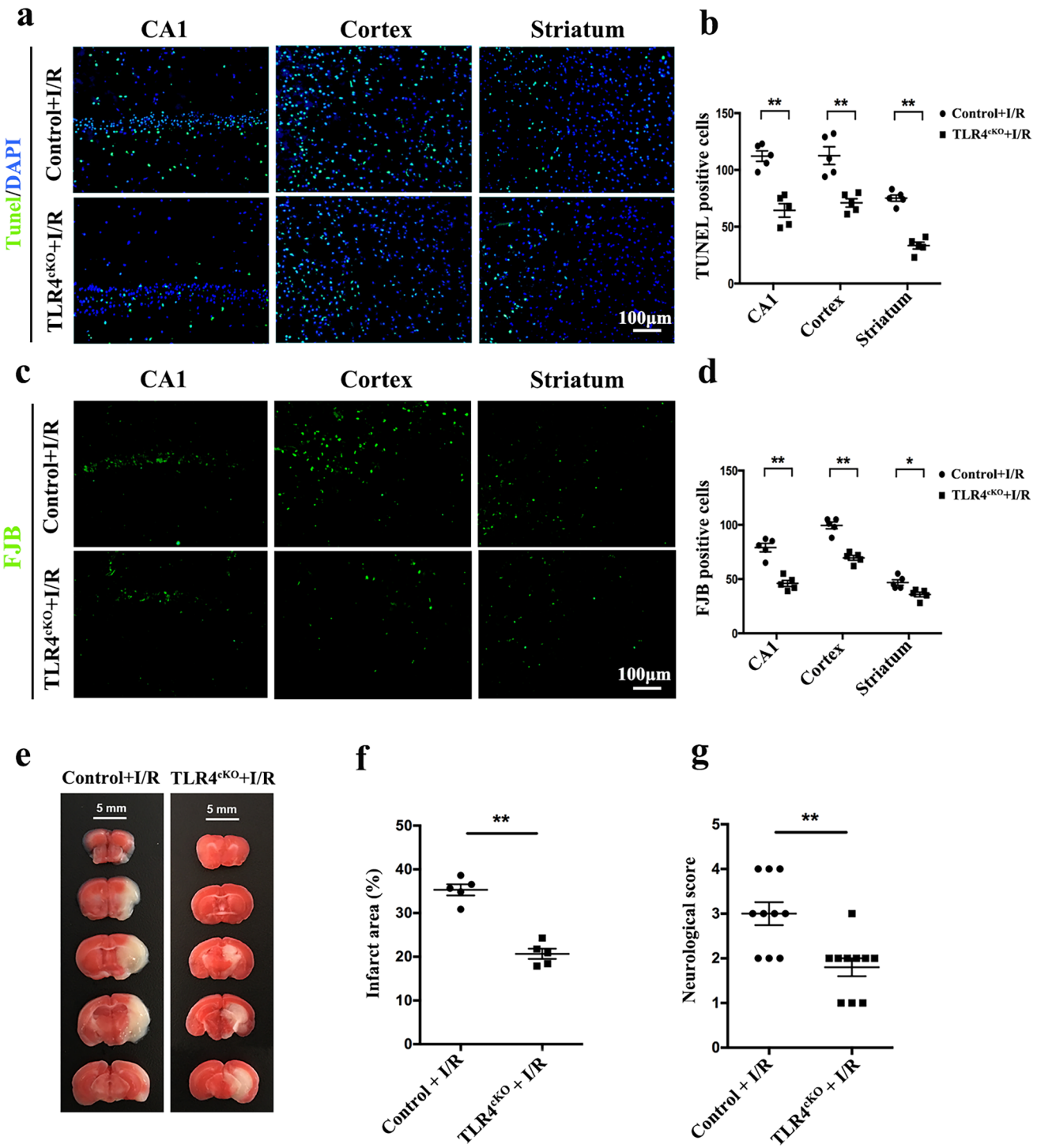

Fig. 2 Deletion of TLR4 from glutamatergic neurons protects neurons from ischemic damage and improves functional deficits in a mouse stroke model. **a–d** Images of the cortex, striatum, and hippocampus from TLR4^{cKO} (Vglut2$^{ires-Cre/+}$ + Tlr4$^{fl/fl}$) and control (Tlr4$^{fl/fl}$) mice that were stained with TUNEL (**a**) and Fluoro-Jade B (FJB) (**c**) 24 h after ischemia/reperfusion (I/R). Bar graphs show summarized TUNEL-labeled (**b**) and FJB-labeled (**d**) cells ($n = 5$). **e** Images of brain sections from TLR4.^{cKO} and control mice 24.5 h after I/R were stained with TTC. **f**, **g** Bar graphs show infarct volumes (**f**) ($n = 5$) and neurological scores (**g**) ($n = 10$) for mice subjected to I/R. Values are represented as the mean ± SEM. $^{*}P < 0.05$, $^{**}P < 0.01$

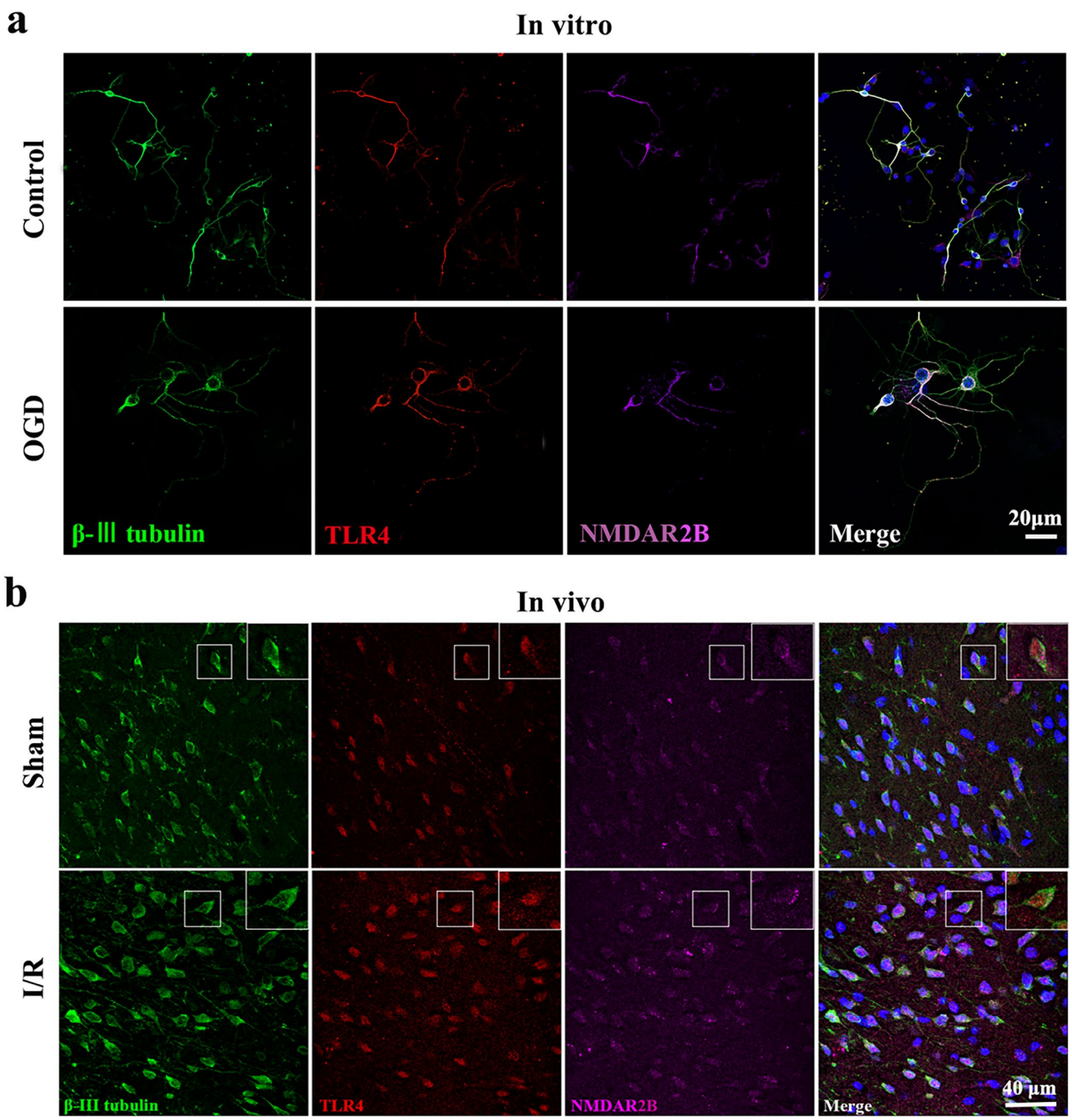

Fig. 3 Colocalization of TLR4 and NMDAR2B in neurons respond to ischemic stimulation. **a**, **b** Representative immunofluorescence photomicrographs showing the colocalization of NMDAR2B (purple) and TLR4 (red) in neurons (green) in vitro (**a**) and in vivo (**b**) following OGD and I/R, respectively

Deletion of TLR4 from Vglut2 Neurons Attenuates Middle Cerebral Artery Occlusion/Reperfusion-Induced Phosphorylation of NMDAR2B and nNOS–PSD-95 Interaction

We next investigated the effects of deletion of TLR4 from Vglut2 neurons on NMDAR2B-mediated toxicity following I/R injury in vivo. The Western blot results of tissue samples taken from the ischemic cortex demonstrated that deletion of TLR4 in glutamatergic neurons decreased the levels of p-NMDAR2B and nNOS following I/R injury (Fig. 5a–c) but had no effect on the level of Src kinase (Fig. 5d), which is consistent with the in vitro results.

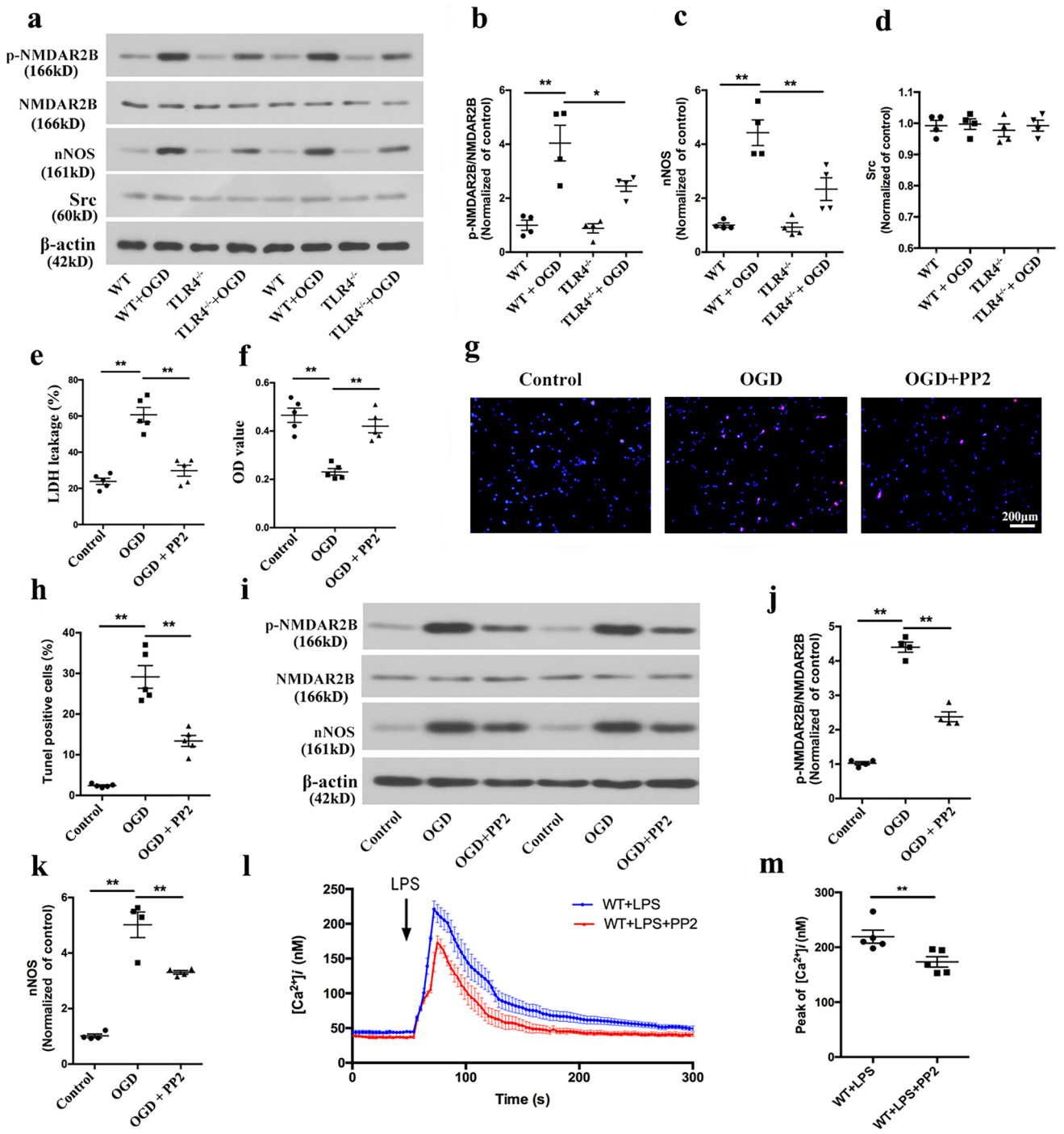

Fig. 4 Involvement of Src kinase and the NMDAR2B phosphorylation axis in TLR4-mediated neuronal death following OGD and LPS-induced intracellular Ca^{2+} increase. **a** Immunoblot analysis of proteins in cell lysates of neurons from WT and TLR4 knockout mice following exposure to OGD. **b–d** Bar graphs show the levels of phosphorylation at Ser-1303 (p-NMDAR2B)/NMDAR2B (**b**), nNOS (**c**), and Src kinase (**d**) ($n=4$). **e**, **f** PP2, an inhibitor of the Src family of protein kinases, effectively decreased lactate dehydrogenase (LDH) release (**e**) and increased cell viability (**f**) following OGD ($n=5$). **g**, **h** Cell survival was quantified using TUNEL staining following PP2 and OGD treatments ($n=5$). **i** Blots showing NMDAR2B, p-NMDAR2B, and nNOS in cell lysates of neurons following PP2 and OGD treatments. **j**, **k** Bar graphs show the levels of phosphorylation at Ser-1303 (p-NMDAR2B)/NMDAR2B (**j**) and nNOS (**k**) ($n=4$). **l** The average kinetics of Ca^{2+} in the WT + LPS and WT + LPS + PP2 groups ($n=5$). LPS treatment is shown by arrows. **m** Bar graphs represent the peak value of the neuronal Ca^{2+} response for LPS and PP2 treatments ($n=5$). Values are represented as the mean ± SEM. $^{*}P<0.05$, $^{**}P<0.01$

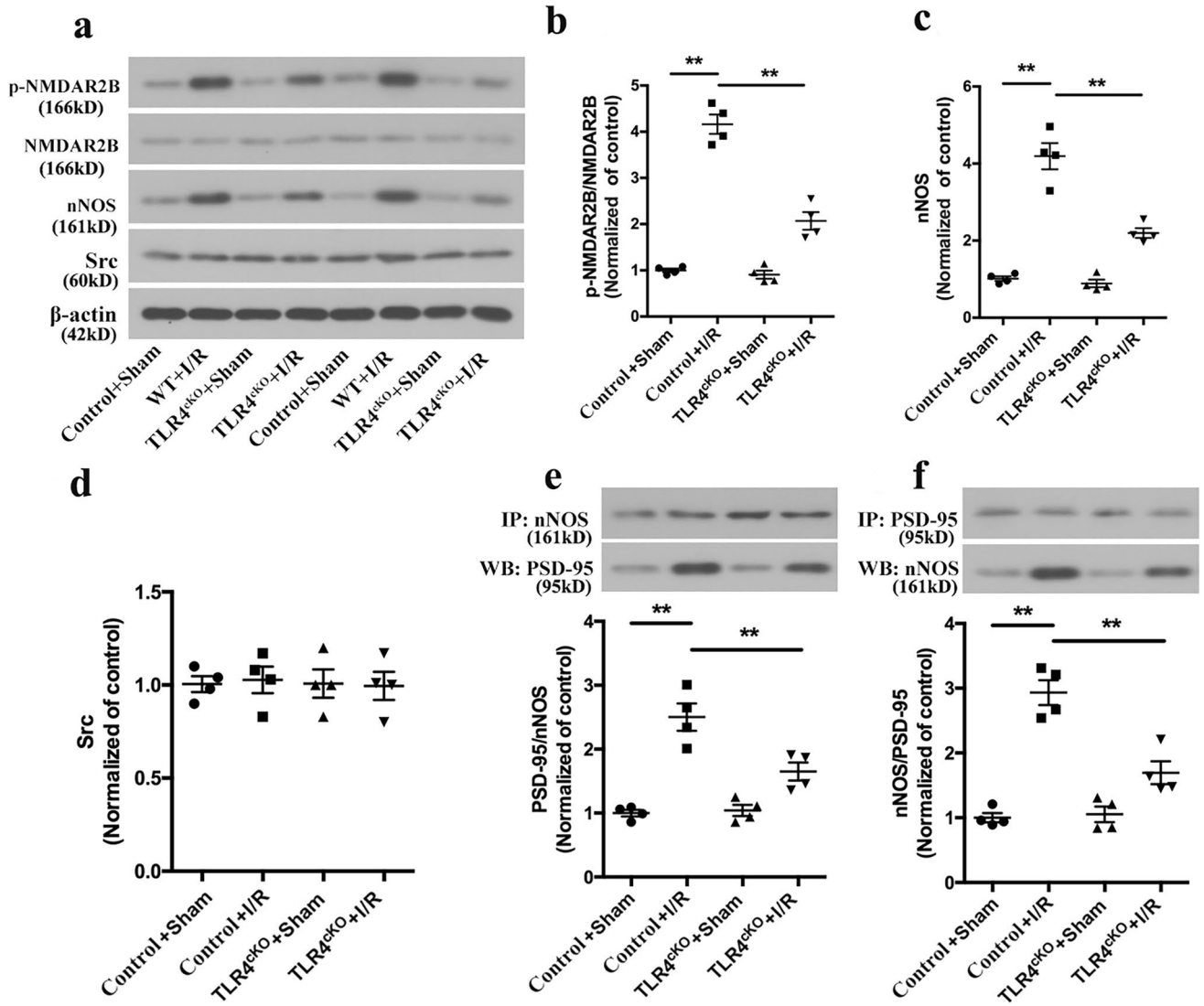

Fig. 5 Deletion of TLR4 from glutamatergic neurons decreases the phosphorylation of NMDAR2B and dissociates the nNOS–PSD-95 interaction in a mouse stroke model. **a** Western blot images of protein bands. **b–d** Quantitative analysis of the levels of phosphorylation at Ser-1303 (p-NMDAR2B)/NMDAR2B (**b**), nNOS (**c**), and Src kinase (**d**) ($n=4$). **e**, **f** Coimmunoprecipitation experiments showing the effect of deletion of TLR4 from glutamatergic neurons on nNOS–PSD-95 interaction after I/R ($n=5$). Values represent the mean ± SEM. $^{**}P<0.01$

Since ischemia-induced neuronal death is caused by NMDAR-dependent nNOS translocation from cytosol to membrane via an nNOS–PSD-95 interaction [27, 28], we performed coimmunoprecipitation experiments with tissue samples taken from the ischemic cortex of mice following MCAO and 24-h reperfusion. The results showed that I/R injury induced a significant increase in the nNOS–PSD-95 complex in control mice, which was significantly prevented in mice with deletion of TLR4 from Vglut2 neurons (Fig. 5e, f). These findings demonstrate that selective elimination of TLR4 in neurons suppresses activation of NMDAR2B-dependent nNOS–PSD-95 interaction and protects neurons against death induced by I/R injury.

Discussion

In this study, we present the novel finding that neuronal TLR4 is essential for ischemia-induced neuronal death via NMDAR2B-mediated toxicity. Selective elimination of TLR4 in glutamatergic neurons leads to resistance to death and attenuates both the neurological deficits and brain infarct volumes caused by MCAO. To the best of our knowledge, this is the first report to present comprehensive evidence to elucidate the possible interactions and roles of neuronal TLR4 and NMDAR2B in the pathogenesis of ischemia/reperfusion injury in vivo and in vitro.

It is well known that TLR4 is widely expressed in a diversity of mammalian immune and nonimmune cells and is present in the brain, including glial cells and neurons [9, 29, 30]. A growing amount of evidence has demonstrated the critical role of TLR4 in glia in neuroinflammation induced by I/R injury [31, 32], but few studies have investigated the role of TLR4 in neurons. Tang et al. [4] first found that TLR4 expression in cerebral cortical neurons was increased in response to I/R injury, and the amount of brain damage and neurological deficits caused by a stroke were significantly lower in TLR4 mutant mice than in WT control mice. However, TLR4 mutant mice were used in that study, and TLR4 was mutated in all of the cells and not restricted to neurons, while in the current study, we used conditional deletion of TLR4 on glutamatergic neurons. Since glutamate release increases and accumulates at synapses following brain ischemia and glutamatergic neurons are believed to play a crucial role in ischemic injury [33, 34], we used Vglut2-ires-Cre knock-in mice to manipulate TLR4 expression in Vglut2 (glutamatergic) neurons to test the effects on I/R injury. Remarkably, conditional deletion of TLR4 from glutamatergic neurons alleviated neuronal death, infarct volume, and functional deficits in mice after I/R injury. These findings indicate that neuronal TLR4 is directly involved in the neuropathology of I/R injury but limits glial TLR4-mediated neuroinflammation. However, it is not clear whether TLR4 on other neurons, such as GABAergic neurons and dopaminergic neurons, is involved in I/R injury, which should be evaluated in future studies.

In the current study, we found that neuronal TLR4 modulated the Ca^{2+} influx evoked in the neuronal cell body by LPS treatment. Previous studies have demonstrated that NMDAR-mediated calcium inflow plays a key role in the development of I/R injury; for example, ischemia-induced neuronal intracellular Ca^{2+} overload and neuronal death are mediated by NMDARs and can be prevented by MK801, an open-channel and use-dependent NMDAR antagonist [35–37]. It is well known that NMDARs play an extremely important role under physiological or pathological conditions, which makes it difficult to safely interfere with NMDARs. In the current study, we surprisingly discovered that activation of neuronal TLR4 following ischemic insult phosphorylated the NMDA receptor NR2B subunit, while conditional deletion of TLR4 in glutamatergic neurons dissociated nNOS–PSD-95 coupling following IRI. The results are important and plausible because NMDAR-dependent nNOS translocation from the cytosol to the membrane via nNOS–PSD-95 interaction has been demonstrated to be the key in ischemia-induced neuronal death [27] and glutamate-induced excitotoxicity [28].

A previous study found that the IL-1β/IL-1R1 axis in neurons increased the phosphorylation of NMADR2B through Src kinase to potentiate Ca^{2+} influx, causing Ca^{2+} overload and neuronal death [24]. Src kinase is involved in Tyr phosphorylation of NMADR2B protein and concomitantly increases the amplitude and duration of NMDAR channel opening [7]. Notably, IL-1R1 and TLR4 share a common cytoplasmic Toll/IL-1 receptor (TIR) domain and can interact with myeloid differentiation factor (MyD88) [25]. In this context, we hypothesized that IL-1R1 and TLR4 on neurons are activated and interact under I/R injury conditions through Src kinase. In line with this proposal, the current results showed that I/R injury induced TLR4-dependent molecular signaling, which modulated the phosphorylation of NMADR2B, NMDA-induced Ca^{2+} response, and ischemic neuronal death through Src kinases. As shown by an experiment, a selective antagonist of Src family kinases was effective against OGD-induced neuronal death. Here, as summarized in Suppl. Fig. S4, our findings indicate that neuronal TLR4 signaling activated Src kinase and promoted the phosphorylation of NMDAR2B, resulting in "Ca^{2+} overload" of neurons, which in turn increased the interaction between PSD95 and nNOS and eventually led to neuronal death following I/R injury.

Conclusions

In conclusion, this is the first report to provide direct evidence for the role of neuronal TLR4 signaling in cerebral ischemic injury, which involves the NMDAR/PSD95-nNOS pathway. Targeting neuronal TLR4 may be a potential neuroprotective therapy for ischemic brain damage.

Supplementary Information The online version contains supplementary material available at https://doi.org/10.1007/s12035-022-03122-9.

Author Contribution L. L., H. S., and T. C. X. conceived the study. Z. A. Z. wrote the main manuscript text, and N. N. Z. and J. L. prepared the figures. H. S. revised the manuscript and language. All authors reviewed the manuscript.

Funding The work was supported by grants from the National Natural Science Foundation of China (No. 81901217) and the Doctoral Research Start-up Foundation of Liaoning (2019-BS-269).

Data Availability The datasets used and/or analyzed during the present study are available from the corresponding author on reasonable request.

Declarations

Ethics Approval and Consent to Participate All experimental procedures were performed in accordance with approved principles of the Animal Ethics Committee of the General Hospital of Northern Theater Command.

Consent for Publication Not applicable.

Competing Interests The authors declare no competing interests.

References

1. Leitner GR et al (2019) Targeting toll-like receptor 4 to modulate neuroinflammation in central nervous system disorders. Expert Opin Ther Targets 23(10):865–882
2. Buchanan MM, Hutchinson M, Watkins LR, Yin H (2010) Toll-like receptor 4 in CNS pathologies. J Neurochem 114(1):13–27
3. Luo L et al (2022) Intermittent theta-burst stimulation improves motor function by inhibiting neuronal pyroptosis and regulating microglial polarization via TLR4/NFkappaB/NLRP3 signaling pathway in cerebral ischemic mice. J Neuroinflammation 19(1):141
4. Tang SC et al (2007) Pivotal role for neuronal Toll-like receptors in ischemic brain injury and functional deficits. Proc Natl Acad Sci USA 104(34):13798–13803
5. Lipton SA (2006) Paradigm shift in neuroprotection by NMDA receptor blockade: memantine and beyond. Nat Rev Drug Discov 5(2):160–170
6. Granzotto A et al (2022) Long-term dynamic changes of NMDA receptors following an excitotoxic challenge. Cells 11(5):911
7. Yu XM, Askalan R, Keil GJ 2nd, Salter MW (1997) NMDA channel regulation by channel-associated protein tyrosine kinase Src. Science 275(5300):674–678
8. Calvo-Rodriguez M et al (2017) Aging and amyloid beta oligomers enhance TLR4 expression, LPS-induced Ca(2+) responses, and neuron cell death in cultured rat hippocampal neurons. J Neuroinflammation 14(1):24
9. Balosso S, Liu J, Bianchi ME, Vezzani A (2014) Disulfide-containing high mobility group box-1 promotes N-methyl-d-aspartate receptor function and excitotoxicity by activating Toll-like receptor 4-dependent signaling in hippocampal neurons. Antioxid Redox Signal 21(12):1726–1740
10. Wang PF et al (2014) Polyinosinic-polycytidylic acid has therapeutic effects against cerebral ischemia/reperfusion injury through the downregulation of TLR4 signaling via TLR3. J Immunol 192(10):4783–4794
11. Thatipamula S, Hossain MA (2014) Critical role of extracellularly secreted neuronal pentraxin 1 in ischemic neuronal death. BMC Neurosci 15:133
12. Tu W et al (2010) DAPK1 interaction with NMDA receptor NR2B subunits mediates brain damage in stroke. Cell 140(2):222–234
13. Cao CX et al (2007) Reduced cerebral ischemia-reperfusion injury in Toll-like receptor 4 deficient mice. Biochem Biophys Res Commun 353(2):509–514
14. Tsien RY, Pozzan T, Rink TJ (1982) T-cell mitogens cause early changes in cytoplasmic free Ca2+ and membrane potential in lymphocytes. Nature 295(5844):68–71
15. Rahmati M, Taherabadi SJ (2021) The effects of exercise training on Kinesin and GAP-43 expression in skeletal muscle fibers of STZ-induced diabetic rats. Sci Rep 11(1):9535
16. Rahmati M, Rashno A (2021) Automated image segmentation method to analyse skeletal muscle cross section in exercise-induced regenerating myofibers. Sci Rep 11(1):21327
17. Duan CM et al (2020) SRT2104 attenuates chronic unpredictable mild stress-induced depressive-like behaviors and imbalance between microglial M1 and M2 phenotypes in the mice. Behav Brain Res 378:112296
18. Ma Y et al (2006) Toll-like receptor 8 functions as a negative regulator of neurite outgrowth and inducer of neuronal apoptosis. J Cell Biol 175(2):209–215
19. Ludhiadch A, Sharma R, Muriki A, Munshi A (2022) Role of calcium homeostasis in ischemic stroke: a review. CNS Neurol Disord Drug Targets 21(1):52–61
20. Wang J et al (2003) Cdk5 activation induces hippocampal CA1 cell death by directly phosphorylating NMDA receptors. Nat Neurosci 6(10):1039–1047
21. Wu QJ, Tymianski M (2018) Targeting NMDA receptors in stroke: new hope in neuroprotection. Mol Brain 11(1):15
22. Salter MW, Kalia LV (2004) Src kinases: a hub for NMDA receptor regulation. Nat Rev Neurosci 5(4):317–328
23. Dawson VL et al (1996) Resistance to neurotoxicity in cortical cultures from neuronal nitric oxide synthase-deficient mice. J Neurosci: Off J Soc Neurosci 16(8):2479–2487
24. Viviani B et al (2003) Interleukin-1beta enhances NMDA receptor-mediated intracellular calcium increase through activation of the Src family of kinases. J Neurosci: Off J Soc Neurosci 23(25):8692–8700
25. O'Neill LA, Bowie AG (2007) The family of five: TIR-domain-containing adaptors in Toll-like receptor signalling. Nat Rev Immunol 7(5):353–364
26. Hanke JH et al (1996) Discovery of a novel, potent, and Src family-selective tyrosine kinase inhibitor Study of Lck- and FynT-dependent T cell activation. J Biol Chem 271(2):695–701
27. Sattler R et al (1999) Specific coupling of NMDA receptor activation to nitric oxide neurotoxicity by PSD-95 protein. Science 284(5421):1845–1848
28. Zhou L et al (2010) Treatment of cerebral ischemia by disrupting ischemia-induced interaction of nNOS with PSD-95. Nat Med 16(12):1439–1443
29. Sadat-Hatamnezhad L, Tanomand A, Mahmoudi J, SandoghchianShotorbani S (2016) Activation of Toll-like receptors 2 by high-mobility group box 1 in monocytes from patients with ischemic stroke. Iran Biomed J 20(4):223–8
30. Li Y et al (2021) Food reward depends on TLR4 activation in dopaminergic neurons. Pharmacol Res 169:105659
31. Famakin BM, Vemuganti R (2020) Toll-like receptor 4 signaling in focal cerebral ischemia: a focus on the neurovascular unit. Mol Neurobiol 57(6):2690–2701
32. Wang Y, Ge P, Zhu Y (2013) TLR2 and TLR4 in the brain injury caused by cerebral ischemia and reperfusion. Mediators Inflamm 2013:124614
33. Zhang P et al (2022) Neuroprotective effects of TRPM7 deletion in parvalbumin GABAergic vs. glutamatergic neurons following ischemia. Cells 11(7):1178
34. Wang F, Xie X, Xing X, Sun X (2022) Excitatory synaptic transmission in ischemic stroke: a new outlet for classical neuroprotective strategies. Int J Mol Sci 23(16):381
35. Mari Y, Katnik C, Cuevas J (2010) ASIC1a channels are activated by endogenous protons during ischemia and contribute to synergistic potentiation of intracellular Ca(2+) overload during ischemia and acidosis. Cell Calcium 48(1):70–82
36. Lipton SA, Rosenberg PA (1994) Excitatory amino acids as a final common pathway for neurologic disorders. N Engl J Med 330(9):613–622
37. Weilinger NL et al (2016) Metabotropic NMDA receptor signaling couples Src family kinases to pannexin-1 during excitotoxicity. Nat Neurosci 19(3):432–442